Calibration errors on experimental slant total electron content determined with GPS

L. Ciraolo[1], F. Azpilicueta[2], C. Brunini[2,3], A. Meza[2,3], S. M. Radicella[4]

1) Istituto di Fisica Applicata 'Nello Carrara' del Consiglio Nazionale delle Ricerche, Via Panciatichi, 64, Firenze, Italia.

2) Facultad de Ciencias Astronómicas y Geofísicas, Universidad Nacional de La Plata, Paseo del Bosque, 1900, La Plata, Argentina

3) Consejo Nacional de Investigaciones Científicas y Tecnológicas, Argentina

4) Aeronomy and Radiopropagation Laboratory, Abdus Salam International Centre for Theoretical Physics, Strada Costiera 11, 34014, Trieste, Italy

Corresponding author's information

Francisco Azpilicueta

e-mail: azpi@fcaglp.unlp.edu.ar

Phone: +54 – 221-4236593/4

Fax: +54 – 221-423-6591

Abstract

The Global Positioning System (GPS) has become a powerful tool for ionospheric studies. In addition, ionospheric corrections are necessary for augmentation systems required for Global Navigation Satellite Systems use. Dual-frequency carrier-phase and code-delay GPS observations are combined to obtain ionospheric observables related to the slant total electron content (sTEC) along the satellite-receiver line-of-sight. This observable is affected by inter-frequency biases (IFB, often called differential code biases, DCB) due to the transmitting and the receiving hardware. These biases must be estimated and reduced from the data in order to calibrate the experimental sTEC obtained from GPS observations. For calibration purposes it is assumed that IFB stay constant over 1-3 days.

Based on the analysis of single differences of the ionospheric observables obtained from pairs of co-located GPS receivers, this research addresses two major issues: 1) assessing the errors translated from

the code-delay to the carrier-phase ionospheric observable by the so-called levelling process applied to reduce carrier-phase ambiguities from the data; and 2) assessing the short-term stability of receiver IFB. The outstanding conclusions achieved are: 1) the levelled carrier-phase ionospheric observable is affected by a systematic error produced by code-delay multi-path through the levelling procedure; and 2) receiver IFB may experience significant changes during one day. The magnitude of both effects depends on the receiver/antenna configuration. Levelling errors found in this research vary from 1.4 to 5.3 total electron content units (TECu). Beside, intra-day variations of code-delay receiver IFB as large as 8.8 TECu were detected.

Key words: Total Electron Content (TEC), GPS, inter-frequency bias, differential code bias (DCB), levelling carrier to code TEC.

1. Introduction

The Global Positioning System (GPS) has become a tool routinely used to investigate the Earth's ionosphere. An important contribution to ionospheric studies based on Global Navigation Satellite Systems (GNSS) has been done by the International GNSS Service (IGS) (Beutler at al. 1999). Throughout the last decade, IGS supported a worldwide effort to deploy and maintain operational a global network of GNSS receivers, whose observations have been used by many scientists for a great variety of ionospheric studies (e.g. Gao et al. 1994; Feltens 1998; Mannucci et al. 1998; Hernández-Pajares et al. 1999; Schaer, 1999). In addition, IGS established in 1998 an Ionospheric Working Group (Hernandez Pajares 2004) that plays an important role in promoting and coordinating ionospheric studies based on GNSS observations. The outstanding information retrieved from GNSS observations is the 3-dimensional (time, longitude and latitude) distribution of the vertical total electron content (e.g. Brunini et al. 2004, Azpilicueta et al. 2005). Total Electron Content (TEC) is defined as the integral of the electron density along a trajectory, usually, the vertical from the Earth surface up to a

given height in the ionosphere (hence, vertical or vTEC) or the line-of-sight from the satellite to the receiver (slant or sTEC). TEC is measured in TEC units (TECu), 1 TECu being 10^{16} electrons/m^2.

The ionospheric delay constitutes the main source of error for GNSS single frequency operation. The sensitivity of the ionospheric range delay to sTEC for the primary GPS signal is 0.162 m per TECu. Hence, the range delay for this signal can reach as much as 90 m for a low elevation satellite (e.g. Langley 1996). An outstanding application of ionospheric models are the so called augmentation systems, which encompass a variety of services developed to provide the user (particularly in civilian aviation) with corrections that attenuate the ionospheric and other navigational errors (Walter et al. 2004). Examples of operational or nearly operational services are the Wide Area Augmentation System (WAAS) in the USA and Canada, the European Geostationary Navigation Overlay System (EGNOS) and the Multifunctional Transport Satellite Space Based Augmentation System (MSAS) in Japan. The necessity of extending such services to other regions of the world with different ionospheric conditions (Central and South America, Africa, India, and China, etc.) has raised the interest of many scientists on GNSS-based ionospheric models.

In a good approximation, the refractivity of the ionospheric plasma for GNSS signals is directly proportional to the electron density and inversely proportional to the square of the signal frequency. Based on this property, the subtraction of simultaneous observations made at different frequencies allows to obtain an ionospheric observable related to the satellite-receiver sTEC (e.g. Leitinger and Putz 1988). This ionospheric observable can be obtained from either carrier-phase or code-delay measurements. Carrier-phase observations are much less affected by measurement noise and multi-path than code-delay observations, but they present the problem of being biased by unknown ambiguities (e.g. Manucci et al. 1999). A widely used procedure to reduce the ambiguities from the carrier-phase ionospheric observable is the so-called “levelling carrier to code” algorithm (see next section). One objective of this paper is to investigate the presence of systematic errors in the carrier-phase ionospheric observable due to that algorithm.

Early investigations concerning sTEC determination with GPS pointed out the existence of systematic delays produced by both transmitter and receiver hardware (e.g., Lanyi and Roth 1988, Gaposchkin and Coster 1992, Sardon et al. 1994, Davies and Hartmann 1997). Because these delays are different from the frequency to frequency (and from the carrier-phase to code-delay observations), an inter-frequency bias (IFB) remains present in the ionospheric observable after subtracting observations at different frequencies. Satellite and receiver IFB combined might reach several tens of nanoseconds or, equivalently, one hundred TECu, therefore their effect has to be removed from the ionospheric observable in order to obtain unbiased sTEC estimates. Usually, satellite and receiver IFB and sTEC are simultaneously estimated from the observations. To separate sTEC from IFB, the spatial and temporal variability of sTEC is represented by means of a variety of approaches (e.g. Ma et al. 2005, Brunini et al. 2003, Otsuka et al. 2002, Jakowski et al. 1996), while IFB are assumed to be constant for a given period of time, usually 1-3 days (Bishop et al. 1994, Sardon and Zarraoa 1997, Brunini et al. 2005). A second scope of this paper is to assess the short-term temporal variability of receiver IFB.

2. Ionospheric observable

The ionospheric observable has been discussed extensively in the literature (e.g. Mannucci et al. 1999 and references therein). It is obtained based on the fact that the effect that the ionosphere produces in the GPS observations depends on the signal frequency

$$I = \alpha \frac{sTEC}{f^2}, \tag{1}$$

where I is the ionospheric range delay at frequency f and α is a constant to convert from TECu to length units. Hence, subtraction of simultaneous observations at different frequencies gives rise to an observable in which all frequency-independent effects (e.g. the satellite-receiver geometrical range, clock errors, tropospheric delay, etc.) disappear but the ionospheric and any other frequency-dependent effects remain present

$$\breve{L}_{I,arc} = \breve{L}_1 - \breve{L}_2 = I_1 - I_2 + c(\tau_{R1} - \tau_{R2}) + c(\tau_1^S - \tau_2^S) + {}^{c}\!/_{f_1} N_{1,arc} - {}^{c}\!/_{f_2} N_{2,arc} + \breve{\varepsilon}_L \,, \quad (2)$$

where sub-indexes 1 and 2 refer to the GPS carriers L1 and L2 and sub-index *arc* refers to every continuous arc of carrier-phase observations (i.e. a group of consecutive observations along which both L1 and L2 ambiguities do not change); c is the speed of light in vacuum; $\breve{L}$ are the carrier-phase measurements expressed in length units; τ_R and τ^S are frequency-dependent biases attributed to delays produced by the receiver and the satellite hardware respectively, expressed in time unities; N are the integer carrier phase ambiguities; and $\breve{\varepsilon}_L$ is the combination of observational noise and multi-path in L1 and L2 carrier-phase observations.

By using Eq. (1), Eq. (2) can be converted into

$$L_{I,arc} = sTEC + B_R + B^S + C_{arc} + \varepsilon_L \,, \quad (3)$$

$L_{I,arc}$ is the ionospheric observable; $B_R = {}^{c}\!/_{\beta}(\tau_{R1} - \tau_{R2})$ and $B^S = {}^{c}\!/_{\beta}(\tau_1^S - \tau_2^S)$ are the so-called satellite and receiver inter-frequency biases (IFB) for carrier-phase observations; $C_{arc} = {}^{c}\!/_{\beta f_1} N_{1,arc} - {}^{c}\!/_{\beta f_2} N_{2,arc}$ is the bias produced by carrier-phase ambiguities in the ionospheric observable; and $\varepsilon_L = {}^{\breve{\varepsilon}_L}\!/_{\beta}$ is the effect of noise and multi-path; it should be noted that all terms of Eq. (3) are expressed in TECu. The constant β, to convert from length to TECu, is defined by $\beta = \alpha\left({}^{1}\!/_{f_1^2} - {}^{1}\!/_{f_2^2}\right)$ ($\beta \cong 0.1$ m/TECu).

Dual-frequency P code-delay observations give rise to an analogous ionospheric observable

$$P_I = sTEC + b_R + b^S + \varepsilon_P \,, \quad (4)$$

where the meaning of the terms is analogous to Eq. (3) with the following differences: P_I is obtained subtracting $\breve{P}_1$ from $\breve{P}_2$ (the ionospheric range delay for code-delay observations have opposite sign than for carrier-phase); satellite and receiver IFB for code-delay (b_R and b^S) are different than those

for carrier-phase; there is not any ambiguity term for code-delay; and the effect of noise and multi-path for code-delay observations, ε_P, is around 100 time greater than for carrier-phase observations (Braasch 1996). SEE ALSO MORE RECENT LITERATURE LIKE PAPERS BY P.BONA AND P. DE JONGE (TU DELFT) AND K. BORRE (UNIVERSITY OF AALBORG)

Once both ionospheric observables have been obtained from carrier-phase and code-delay observations, the ambiguity term for every continuous arc is estimated by means of the so-called "levelling carrier to code" process

$$\left\langle L_{I,arc} - P_I \right\rangle_{arc} = C_{arc} + B_R - b_R + B^S - b^S - \left\langle \varepsilon_P \right\rangle_{arc}, \qquad (5)$$

where the symbol $\langle \cdot \rangle$ indicates a weighted average of all observations in the continuous arc. It should be noted that Eq. (5) neglects the effect of noise and multi-path on carrier-phase observations. PLEASE, INDICATE THE MAGNITUDES FOR BOTH, WHICH MAY BE REMARKABLY DIFFEREN (FROM 0.1 MM - NOISE - TO FEW CM - MULTIPATH). Then,

$$\tilde{L}_{I,arc} = L_{I,arc} - \left\langle L_{I,arc} - P_I \right\rangle_{arc} = sTEC + b_R + b^S + \left\langle \varepsilon_P \right\rangle_{arc} + \varepsilon_L \qquad (6)$$

subtracting Eq. (5) from Eq. (3), the ambiguity term is reduced from the carrier-phase ionospheric observable, where $\tilde{L}_{I,arc}$ is the carrier-phase ionospheric observable levelled to the code-delay ionospheric observable. Eq. (6) shows that, after the levelling process: 1) the carrier-phase IFB is replaced by the corresponding code-phase IFB (code-delay IFB is often called differential code biase, DCB, in the literature devoted to GPS-based TEC studies); and 2) the levelled carrier-phase ionospheric observable may be affected by noise and multi-path present in the code-delay observations, if these quantities do not average to zero in a continuous arc. It is also important to note that, in deriving Eq. (6) the usual assumption of constant satellite and receiver IFB is applied. This assumption will be revised later in this paper.

3. Methodology

This section describes the procedure applied to assess the effects of systematic errors in the levelled carrier-phase ionospheric observable (Eq. 6). The investigation is based on data from co-located GPS receivers. In this context, the word "co-located" is intended as two receivers separated one from another by few meters, so that the sTEC can be considered equal for both receivers. Under this condition, single differences of data from the same satellite collected simultaneously by two co-located receivers, *A* and *B* (i.e. single differences of the ionospheric observable), yield to Eq. (7) for code-delay and Eq. (8) for carrier-phase levelled to code-delay observations.

$$\Delta P_I = P_{I,A} - P_{I,B} = b_{R,A} - b_{R,B} + \varepsilon_{PA} - \varepsilon_{PB} = \Delta b_R + \Delta\varepsilon_P \,, \tag{7}$$

$$\Delta\tilde{L}_{I,arc} = L_{I,arc,A} - L_{I,arc,B} = b_{RA} - b_{RB} + \left\langle \varepsilon_P \right\rangle_{arc,A} - \left\langle \varepsilon_P \right\rangle_{arc,B} + \varepsilon_{LA} - \varepsilon_{LB} = \Delta b_R + \Delta\left\langle \varepsilon_P \right\rangle_{arc} + \Delta\varepsilon_L \,, \tag{8}$$

where Δ is the "single difference" operator (sTEC and satellite IFB are eliminated by the single difference computation).

Accordingly to Eq. (8), single differences of the levelled carrier-phase ionospheric observable should be equal to a constant, Δb_R, defined as the difference of the IFB of the receivers, independently of the observed satellite. It is expected that the data belonging to different satellite arcs deviate from Δb_R by an arc-dependent quantity, $\Delta\left\langle \varepsilon_P \right\rangle_{arc}$, because: 1) code-delay noise and multiptah effects may not be totally removed by the levelling process and 2) the remaining effect is different on both receivers. In addition, small fluctuations, $\Delta\varepsilon_L$, due to carrier-phase noise and multi-path, should be present in the single differences.

It is difficult to estimate the magnitude of $\Delta\left\langle \varepsilon_P \right\rangle_{arc}$ because it depends on many factors. In principle, it can be assumed that the error of a single-differenced data is $\sqrt{2}$ time greater than the error of a non-differenced data. After Eq. (6), the non-differenced levelled carrier-phase ionospheric observable is affected by an arc-dependent systematic error –hereafter named "levelling error", $\left\langle \varepsilon_P \right\rangle_{arc}$ –, equals to the combined effect of code-delay noise and multi-path averaged along every continuous arc. According to Brunini (1998), the RMS error of code-delay ionospheric data increases exponentially as

satellite elevation decreases, from a fraction of TECu close to the zenith to approximately ±10 TECu at 10º elevation. Measurement noise can be considered a random signal (SEE AGAIN P.BONA, P. DE JONGE AND K. BORRE PAPERS), but multi-path should be treated as a systematic rather than a random signal. In spite of that, and with the hope to obtain a roughly estimate of the levelling error, it will be assumed that the RMS error of random noise and multipath combined effect decreases as the square root inverse of the number of averaged data. (SEE DETAILED COMMENTS) If carrier-phase observations are not affected by cycle slips, a continuous arc may last approximately 6 hours and contain around 700 data (assuming the usual 30 second sampling interval). Further assuming that the expectation value of random noise and multi-path is equal to zero, it follows that the levelling error should not be greater than a fraction of TECu. The analysis that will be presented in the following section indicates the existence of levelling errors much greater than the optimistic "fraction of TECu" previously estimated. The explanation for these large errors might be that the assumption of multipath effect averaging to zero is no valid as is suggested by (Byun et al. 2002).

4. Results

Table 1 summarizes the relevant characteristics of the data set used in this research: four-character station name, receiver and antenna type, approximate longitude and latitude of the receivers and period of time covered by the observations. The receivers belong to the IGS and the EGNOS test bed networks. In addition, a dedicated experiment was performed at La Plata National University (UNLP) with the aim to isolate systematic errors due to other sources than code-delay multi-path. It consisted in a "zero-baseline" experiment (i.e. two receivers, namely LPGB and LPGR, connected to the same antenna via an antenna splitter device). The zero-baseline antenna was set up very close (few meters) to the co-located LPGS and LPG2 receivers (LPGS is the official IGS site while LPG2 was installed at La Plata Observatory to serve the CHAMP mission).

4.1 Analysis of the levelled single differences of the carrier-phase ionospheric data

Fig. 1 shows graphics of single differences of the levelled carrier-phase ionospheric observable (Eq. 8) for different pairs of co-located receivers and for different days (different satellites are represented with different colours). The sampling interval is 30 seconds and the cut-off elevation mask is 10º. The figure shows representative cases of the different situations found in the analysis. A first conclusion extracted from this analysis is that the levelling error –which is inferred from the spread between single differences corresponding to different arcs (PLEASE DETAIL: IT SEEMS TO BE COMPUTED AS THE HALF OF THE SPREAD REDUCED TO UNDIFFERENCED IONOSPHERIC OBSERVABLES BY THE FACTOR OF SQRT(2)) –, is strongly dependent on the antenna/receiver configuration. The upper panels of Fig. 1 show the worst cases found in the sample, both corresponding to the LPGB-LPGS combination. In these cases the arc-to-arc spread reaches a peak-to-peak value of almost 15 TECu, which leads to levelling errors as large as $\left(15 \quad 2\right) \; 2 \simeq 5.3$ TECu. Complementary, bottom panels of Fig. 1 show the best cases found in the sample, both corresponding to the LPGS-LPG2 combination (same receiver/antenna configuration). In these cases the peak-to-peak spread is lower than 4 TECu, which leads to levelling errors of approximately 1.4 TECu. It should be noted, however, that the actual levelling error could be larger that this value, because an identical receiver/antenna configuration may introduce correlation between the errors of non-differenced data.

Another conclusion extracted from the analysis of the sample is that, for some days, single differences of levelled carrier-phase ionospheric data show an intra-day variation that affects all satellites and arcs in a magnitude that depends on the receiver/antenna configuration. This variation is truly apparent on day 188 for the LPGB-LPGS configuration (upper-left panel of Fig. 1), as an inverted “U-shape” with peak-to-peak range of almost 25 TECu. For the same day, a less pronounced variation with peak-to-peak range of about 4 TECu is also present for the LPGS-LPG2 configuration (bottom-left panel). On day 189, the variation is neither evident for LPGB-LPGS (upper-right panel) nor for LPGS-LPG2 (bottom-right panel) configurations. After Eq. (8) follows that this variation should be attributed to instabilities of the code-delay IFB of both receivers, combined through the single difference operation in the term Δb_R. Assuming that the variations of both receivers are uncorrelated, it can be inferred that in one day a code-delay receiver IFB can change as much as $\left(25 \quad 2\right) \; 2 \simeq 8.8$ TECu.

In summary, two different processes have been discussed: 1) an arc-dependent levelling error attributed to systematic effects of code-delay multi-path that do not cancel after averaging the data for a continuous arc; and 2) an intra-day variation of the code-delay receiver IFB that is present some days but others is not. The analysis performed shows that the magnitude of both effects is dependent on the receiver/antenna configurations. Particularly, both effects achieve the largest values when a NovAtel receiver/antenna configuration is involved in the co-located pair.

In order to substantiate the hypothesis that levelling errors are produced by code-delay multi-path, single differenced levelled carrier-delay ionospheric data from the zero-baseline experiment involving the LPGB and LPGR receivers are analyzed. Fig. 2 shows the corresponding results for the same days previously shown in the upper panels of Fig. 1. It is noticeable the reduction of the arc-to-arc spread (up to a peak-to-peak value lower than 2 TECU). This fact is taken as evidence in favour of multi-path, as the cause of the levelling error. It is also noticeable that the temporal variation of code-delay receiver IFB present on day 188 for the LPGB-LPGS configuration (upper-left panel of Fig. 1) is drastically reduced (even if it does not disappear completely) in the zero-baseline experiment (left panel of Fig. 2). This fact indicates that the major part of it should be produced by instabilities of the NovAtel antenna and/or by some hardware or firmware instability that behaves almost identically for the two NovAtel receivers.

4.2 Analysis of code-delay multi-path effect and the instabilities of the code-delay receiver IFB

From the analysis previously presented, it follows that the arc-to-arc spread and the intra-day variation of the levelled carrier-phase ionospheric observable are both produced in the levelling process by residual effects of code-delay multi-path and by instabilities in the code-delay receiver IFB. Thus, the origin of both problems should be traced back in code-delay rather than in carrier-phase data. The following analysis, based on the code-delay ionospheric observable (Eq. 7) instead of the levelled

carrier-phase ionospheric observable (Eq 8), is presented in order to confirm this assertion. Fig. 3 is analogue to Fig. 1, but obtained from smoothed code-delay data. The reason for data smoothing is to attenuate the effect of the large random noise that affects the code-delay ionospheric observations, thus recovering any underlying systematic signals. It was achieved by applying the following procedure: firstly, a cut-off elevation mask of 60º was imposed in order to discard low-elevation data; then, a low-pass filter based on a moving average was applied in order to reduce high-frequency effects of random noise. The window of the low-pass filter was empirically adopted. After several trials, it was found that an 8-minutes moving average significantly reduces the scatter of the plots, but preserves the systematic patterns that are characteristic of the multi-path signal. Even though the scatter of the plots has largely increased, the relevant behaviours of Fig. 1 (i.e. the arc-to-arc spread and the intra-day variability) can be easily recognized in Fig. 3. This fact confirms the assertion about the code-delay origin of the spread and the intra-day variability observed in the carrier-phase single differences graphics.

Since the relative position of the satellites, receiving antennas and objects that can produce signal reflections and diffractions repeats after one sidereal day, multi-path effect is characterized by a pattern that repeats with one sidereal day period (Braasch 1996). If levelling error is effectively produced by code-delay multi-path, the single-differences of the code-delay ionospheric observable for a given satellite should exhibit a systematic pattern shifted by approximately 4 minutes from one day to the following. This behaviour was effectively confirmed for all samples described in Table 1. Fig. 4 shows the results obtained for one particular satellite and for two particular pairs of co-located receivers (LPGB-LPGS in the left panel and POTS-POTM in the right one). The figure shows four lines, representing the single-differenced code-delay ionospheric observable corresponding to four consecutive days, represented against Universal Time (upper panel), elevation angle for the ascending and descending satellite trace (middle panels) and satellite azimuth (bottom panel). The fingerprint of multi-path can easily be recognized. It does not make sense to show figures for other satellites or other co-located receiver pairs because all of them lead to similar conclusions than those already reported.

5. Conclusions

Code-delay GPS observations are affected by frequency-dependent systematic biases produced by both the satellites and the receiver. The difference of these biases gives rise to a satellite and a receiver IFB in the code-delay ionospheric observable. These code-delay IFB are later translated to the carrier-phase ionospheric observable, when carrier phase data are levelled to code-delay data in order to reduce the effects of carrier phase ambiguities. Since the combination of satellite and receiver IFB may reach a value as large as 100 TECu, they should be estimated and reduced from the data in order to calibrate the experimental sTEC obtained from GPS observations. For calibration purposes it is often assumed that both satellite and receiver code-delay IFB are constant during 1-3 days. This research focused on two major issues: 1) to assess the errors translated from the code-delay to the carrier-phase ionospheric observable by the levelling process; and 2) to assess the intra-day stability of code-delay receiver IFB. The research was based on the analysis of single differenced ionospheric observable obtained from pairs of co-located GPS receivers. The outstanding conclusions are summarized in the following paragraphs.

The levelled carrier-phase ionospheric observable is affected by systematic errors whose effects do not cancel after averaging all the data in a continuous arc. Different experiments are being conducted with the aim to isolate the cause of these errors. Results showed in this paper allow to speculate that code-delay multi-path is the main contributor to levelling errors. Even for the same satellite, two different arcs are generally affected by different levelling errors. Hence, the code-delay ionospheric observable would be better modelled if an arc-dependent bias, $\tilde{b}_{arc}$, is included in Eq. (4), instead of a receiver-dependent IFB, b_R. Such arc-dependent bias, $\tilde{b}_{arc}$, should account for receiver-dependent IFB, b_R, and for the arc-dependent levelling error, $\langle \varepsilon_P \rangle_{arc}$.

Code-delay receiver IFB can be affected by significant intra-day variations. Even for the case of same receiver/antenna configuration, the pattern of the difference of the IFB for one day can be significantly

different from the pattern of the following day. The cause of this could be associated to changes in the environmental conditions nearby the antenna/receiver.

The magnitude of both effects, levelling errors and intra-day variability of code-delay receiver IFB, is dependent on the receiver/antenna configuration. Levelling errors varying from 1.4 to 5.3 TECu were found in this research. Beside, intra-day variations of code-delay receiver IFB as large as 8.8 TECu were detected.

From the analysis presented in this contribution, we conclude that a proper model of the GPS levelled code-delay ionospheric observable should include: 1) a term that does not cancel out when averaging over a continuous arc, associated to multipath effect and 2) the receiver IFB should be consider as a time-varying term.

References

Azpilicueta F, Brunini C, Radicella SM (2005) Global ionospheric maps from GPS observations using modip latitude. Advaneces in Space Research, JASR 7882,8 pp., in press.

Beutler G, Rotacher M, Schaer, Springer TA, Kouba J, Neilan RE (1999) The International GPS Service (IGS): an interdisciplinary service in support of earth sciences. Advances in Space Research 23(4): 631-653.

Bishop G, Walsh D, Daly P, Mazzella A, Holland E (1994) Analysis of the temporal stability of GPS and GLONASS group delay correction terms seen in various sets of ionospheric delay data. Proc. ION GPS-94, pp 1653-1661.7.

Braasch M (1996) Multipath effects. In: Global Positioning System: theory and applications, vol 1. Parkinson BW Spilker JJ (eds) American Institute of Aeronautics and Astronautics, pp 547-568.

Brunini C, Meza A, Bosch W (2005) Temporal and spatial variability of the bias between TOPEX- and GPS-derived total electron content. J. Geodesy 79, doi: 10.1007/s00190-005-0448-z.

Brunini C, Meza A, Azpilicueta F, Van Zele A, Gende M, Diaz A (2004) A new ionosphere monitoring technology based on GPS. Astrophysics and Space Science 290: 415-429.

Brunini C, Van Zele MA, Meza A, Gende M (2003) Quiet and perturbed ionospheric representation according to the electron content from GPS signals. J Geophysical Research, 108, doi: A2 10.1029/2002JA009346.

Brunini C (1998) Global Ionospheric model from GPS measurements**.** PhD thesis, Facultad de Ciencias Astronómicas y Geofísicas, Universidad Nacional de La Plata.

Byun SH, Hajj GA, Young LE (2002) De velopment and application of GPS signal multipath simulator. Radio science 37(6), doi:10.1029/2001RS002549.

Coco DS, Coker C, Dahlke SR, Clynch JR (1991) Variability of GPS satellite differential group delays biases. IEEE Transactions on Aerospace and Electronic Systems, 27(6): 931-938.

Davies K, Hartmann GK (1997) Studying the ionosphere with the Global Positioning System . Radio science 32(4): 1695-1703.

Feltens J (1998) Chapman Profile Approach for 3-d Global TEC representation. Proc 1998 IGS Analysis Centres Workshop, Darmstadt, pp 285-297.

Gao Y, Heroux P, Kouba J (1994) Estimation of GPS receiver and satellite L1/L2 signal delay biases using data from CACS. Proc KIS-94, Banff, pp 109-117.

Goposchkin EM, Coster AJ (1992) GPS L1-L2 bias determination. Proc. International Beacon Satellite Symposium, Massachusetts.

Hernandez Pajares M (2004) IGS Ionosphere WG: an overview. Proc. COST 2004, pp. 29-29.

Hernández-Pajares M, Juan JM, Sanz J (1999) New approaches in global ionospheric determination using ground GPS data. J Atmospheric and Solar Terrestrial Physics 61: 1237-1247.

Jakouski N, Sardon E, Egler E, Jungstand A, Klahn D (1996) About the use of GPS measurements for ionospheric studies. In: Beutler G, Hein GW, Melbourne WG, Seebr G (eds) GPS Trends in Precise Terrestrial Airborne and Spaceborne Applications, IAG Symposium 115, Springer, Berlin, Heidelberg, New York, pp 335-340.

Langley R (1996) Propagation of the GPS signals. Kleusberg A, Teunissen P (eds) GPS for geodesy. Springer, Berlin Heidelberg New York, ISBN 3-540-60785-4, pp 103-140

Lanyi GE, Roth T (1988) A comparison of mapped and measured total ionospheric electron content using Global Positioning System and beacon satellite observations. Radio Science, 23: pp. 483–492.

Leitinger R, Putz E (1988) Ionospheric refraction errors and observables. Atmospheric effects on geodetic space measurements. Monograph 12, School of Surveying, University of New South Wales, pp 81-102

Ma XF, Maruyama T, Ma G (2005) Determination of GPS receiver differential biases by neuronal network parameter estimation method. Radio science 40, RS1002, doi:10.1029/2004RS003072.

Manucci AJ, Iijima BA, Lindqwister UJ, Pi X, Sparks L, Wilson BD (1999) GPS and ionosphere. URSI reviews of Radio Science, Jet Propulsion Laboratory, Pasadena.

Mannucci, AJ, Wilson, BD, Yuan DN, Ho CH, Lindqwister UJ, Runge TF (1998) A global mapping technique for GPS-derived ionospheric total electron content measurements. Radio Science 33: 565-582.

Otsuka Y, Ogawa T, Saito A, Tsugawa T, Fukao S, Miyasaky S (2002) A new method for mapping of total electron content using GPS in Japan. Earth Planets Space 54: 63-70.

Sardon E, Rius A, Zarraoa N (1994) Estimation of the transmitter and receiver differential biases and the ionospheric total electron content from Global Positioning System observations. Radio Science 29: 577-586.

Sardon E, Zarraoa N (1997) Estimation of total electron-content using GPS data: how stable are the differential satellite and receiver instrumental biases? Radio Science 32: 1899-1910.

Schaer S (1999) Mapping and predicting the Earth's ionosphere using the Global Positioning System. PhD thesis, Bern University.

Walter T, Blanch J, Rife J (2004) Treatment of Biased Error Distributions in SBAS. Presented at GNSS 2004, The 2004 International Symposium on GNSS/GPS, Sydney.

Station name	*Organization*	*Receiver type*	*Antenna type*	*Lon - Lat*	*Observation period*
LPGS	IGS	(1118) AOA Benchmark ACT 3.3.32.2N	(367) AOAD/M_T	57.9 º W 34.9 º S	2005, days 188 – 191
LPG2	CHAMP	(1135) AOA Benchmark ACT 3.3.32.2N	(508) AOAD/M_T		
LPGB	UNLP	NovAtel Millenium	NovAtel 503		
LPGR	UNLP	NovAtel Millenium			
POTM	CHAMP	(1106) AOA Benchmark ACT 3.3.32.2N	(346) AOAD/M_T	13.1 º E 52.4 º N	2004, days 001 – 030
POTS	IGS	(281-U) AOA SNT-8000 ACT 3.3.32.3	(235) AOAD/M_T		
TLSE	IGS	(30708) TRIMBLE 4000SSI 7.19A	(227554) TRM29659.0	1.5 º E 43.6 º N	2004, day 336 – 2005, day 212
TLSM	EGNOS	(SLG9803) NovAtel Millenium 4.45	(CRG0xxx) ASH701073.1 S		

Table 1. Data set used in this research.

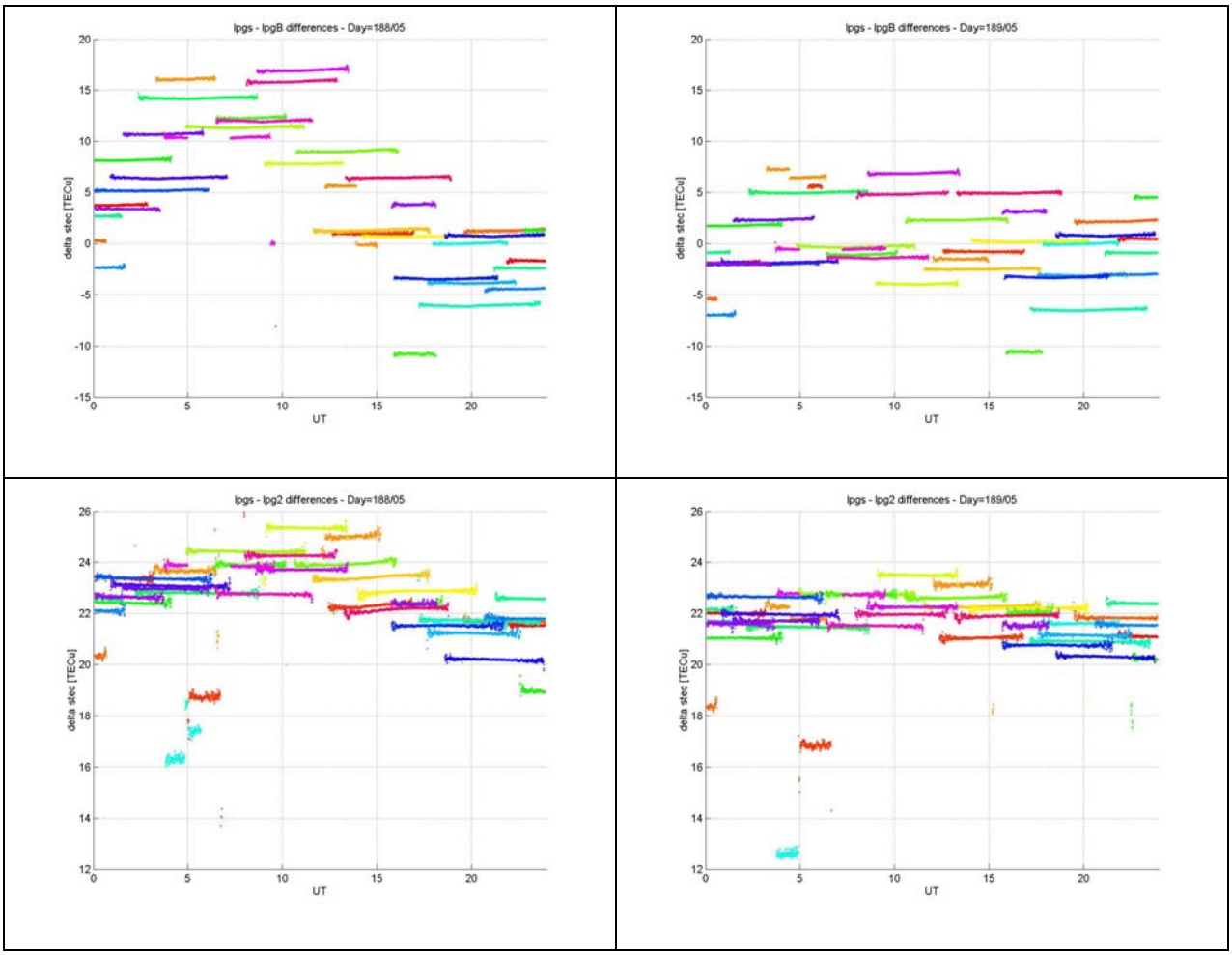

Figure 1. Single differences of the levelled carrier-phase ionospheric observable for different pairs of co-located receivers and different days.

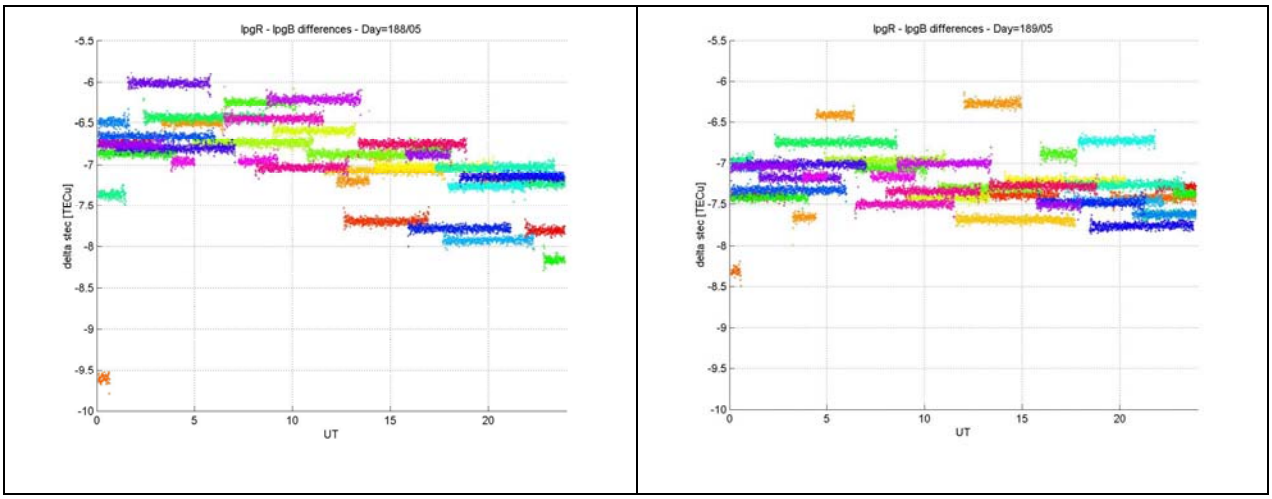

Figure 2. Single differences of the levelled carrier-phase ionospheric observable for the zero-baseline experiment for days 188 and 189.

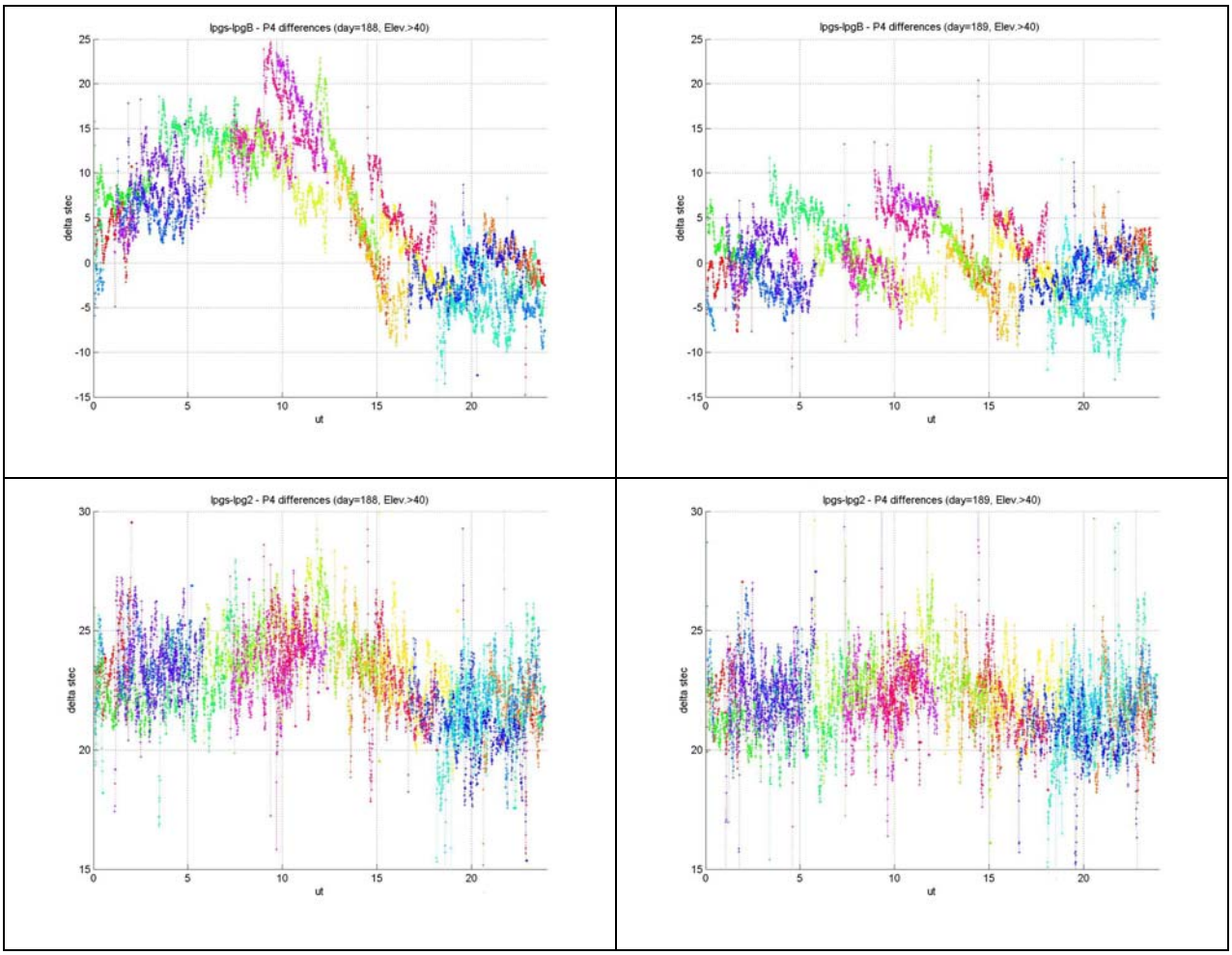

Figure 3. Smoothed single differences of the levelled code-delay ionospheric observable for different pairs of co-located receivers and different days.

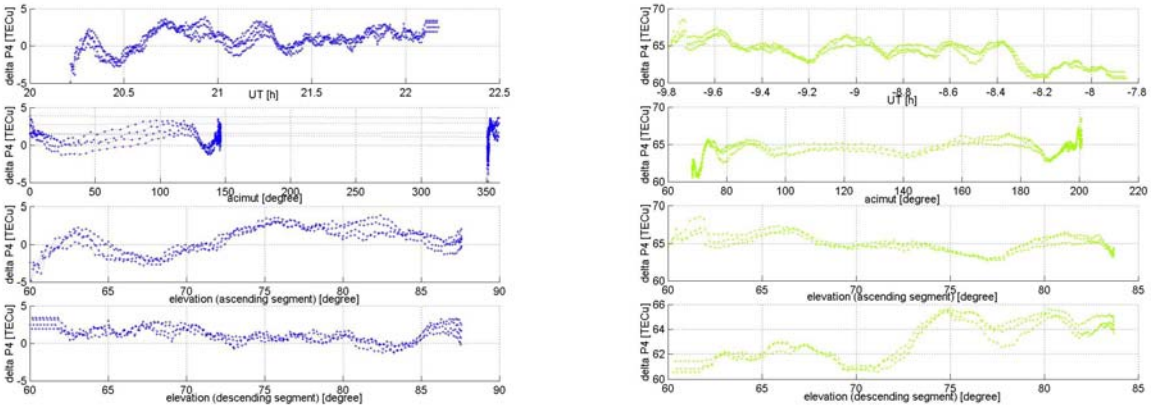

Figure 4. Fingerprint of multi-path in the smoothed single difference of the levelled code-delay ionospheric observable for different pairs of co-located receivers and different days.